PREPARATION AND CHARACTERIZATION OF MESOPOROUS CeO_2-ZrO_2 NANOPOWDERS USING DODECYLAMINE AND SODIUM DODECYL SULFATE AS SURFACTANT

A Dissertation
Submitted in partial fulfillment

FOR THE DEGREE OF

MASTER OF SCIENCE IN CHEMISTRY

Under The Academic Autonomy

NATIONAL INSTITUTE OF TECHNOLOGY, ROURKELA

By

Aniruddha Panda

Under the Guidance of

Dr. Aparna Mondal

DEPARTMENT OF CHEMISTRY
NATIONAL INSTITUTE OF TECHNOLOGY
ROURKELA – 769008, ORISSA

CERTIFICATE

Dr. Aparna Mondal
Department Of Chemistry,
National Institute Of Technology,Rourkela

This is to certify that the dissertation entitled ***"Preparation & Characterization of mesoporous CeO_2-ZrO_2 Nanopowders using Dodecylamine & Sodium Dodecyl Sulfate as Surfactant"*** being submitted by **Aniruddha Panda** to the Department of Chemistry, National Institute of Technology, Rourkela, Orissa, for the award of the degree of Master of Science is a record of bonafide research carried out by him under my supervision and guidance. To the best of my knowledge, the matter embodied in the dissertation has not been submitted to any other University / Institute for the award of any Degree or Diploma.

N.I.T. Rourkela.
Date:

Dr. Aparna Mondal
(Supervisor)

ACKNOWLEDGEMENTS

With deep regards and profound respect, I avail this opportunity to express my deep sense of gratitude and indebtedness to Dr. Aparna Mondal, Department of Chemistry, National Institute of Technology, Rourkela, for introducing the present project topic and for her inspiring guidance, constructive criticism and valuable suggestion throughout the project work. I most gratefully acknowledge her constant encouragement and help in different ways to complete this project successfully.

I would like to acknowledge my deep sense of gratitude to Dr. R. K. Patel, Head, Department of Chemistry, National Institute of Technology, Rourkela, for his valuable advices and constant encouragement for allowing me to use the facilities in the laboratory.

I would also like to thank Dr. B. B. Nayak, Department of Ceramic Engineering, National Institute of Technology, Rourkela, for his help in taking XRD data's. I wish to thank all the faculty members & staff members of Department of Chemistry for their support and help during the project.

Last but not the least, I remember with gratitude my family members who were always a source of strength, support and inspiration.

Rourkela

Date: **(Aniruddha Panda)**

IN THE MEMORY OF MY LATE AUNT
"SADHANA"

ABSTRACT

The present project work deals with the synthesis and characterization of Zr^{4+} doped porous CeO_2 nanopowders, which has high thermal resistance, improved reduction efficiency of the Ce^{4+}/Ce^{3+} redox couple, excellent oxygen storage/release capacity and better catalytic activity at lower temperature than pure ceria. CeO_2-ZrO_2 oxides with different ZrO_2 content (0, 2, 5,10 mol %) were prepared. The work involves a systematic study and analysis of the structures of the samples prepared under different conditions. Mesoporous CeO_2-ZrO_2 nanopowders synthesized in cubic fluorite structure, which is stable up to as high as 500°C using an inorganic salt of zirconium and surfactants of dodecyl amine and sodium dodecyl sulphate. FTIR results show that the mesoporous CeO_2-ZrO_2 nanopowders heated at 500°C is free from surfactant. The results of the porous CeO_2-ZrO_2 formation and their stabilities, phase transformation, crystallite sizes and microstructures are studied with X-ray diffraction, IR analysis, and SEM analysis. The XRD data's showed the as prepared CeO_2-ZrO_2 powder particles have single phase cubic fluorite structure.

Keywords: Cubic fluorite structure; porous CeO_2-ZrO_2; microstructures; crystallite sizes; phase transformations;

TABLE OF CONTENTS

Page

CHAPTER-I

INTRODUCTION

1.1 General Introduction

Porous materials play important roles in many applications, which stimulate the research interest in developing new synthetic methods for new porous materials, especially for those stable over long periods at high temperatures. Since the hexagonally packed mesoporous silicate materials, i.e., the MCM-41 series with uniform pores and large surface areas surpassing 1000 m2/g, were reported in 1992 [1,2] via a surfactant micelle-assisted process, plenty of research works on porous materials have been documented. The method using surfactant micelles as template has also been used for the preparation of various oxide materials other than silica with high surface area and ordered pore systems [3,4]. Among them, mesoporous transition metal oxides are more widely used as solid catalysts [5,6], catalyst supports [7] and host materials [8] for nanocomposites. Unfortunately, the thermal or hydrothermal stability of these mesoporous materials is in many cases less satisfactory compared with the mesoporous silica. The thin walls among the pores and re-crystallization of the oxide walls are the reasons for the low thermal or hydrothermal stabilities. Recent progress in this field shows the method of using nanoparticles as the building blocks is a promising strategy to modify the stabilities of mesoporous materials, in which nanoparticles stack to bulk mesostructures [9–15]. Thus materials prepared are viewed important for many applications such as catalysis and high-surface area materials [16]. Cerium oxide has received considerable research attention for its application in various aspects [17–21]. For example, it can be used as active component in combustion catalyst and as an important additive in three-way catalysts for vehicle emission control [22]. And its unique support effect on loaded catalytic metals has been revealed recently [23]. Using the conventional method, meso-ceria has been reported to collapse easily at mild temperatures [24,25].

1.2 Application of Ceria Based Materials

The very essential and most important use of ceria containing materials is catalytic application in automotive three-way catalysts (TWC) [26] and oxidation catalysts (for example, diesel oxidation catalysts, DOC) because of their oxygen storage capacity (OSC) based on the unique redox behavior between Ce^{3+} and Ce^{4+} [27,28].

CeO_2 is included in materials used in fuel-cell processes [29], in oxygen permeation membrane systems [30], and as catalysts in numerous economically and technologically important industrial processes. The presence of CeO_2 promotes various catalytic reactions such as CO_2 activation, CO oxidation, CO/NO removal, low-temperature water-gas shift [31], the oxidation of different hydrocarbons, wet oxidation processes of organic compounds, the removal of total organic carbon from industrial wastewaters, methane reforming with CO_2, SO_2 reduction with CO. Other significant applications of cerium-containing catalysts include removal of soot from diesel engine exhaust and as an additive for combustion catalysts. It has been reported that ceria has potential uses for the removal of post-combustion pollutants and of high strength organics from wastewater (catalytic wet oxidation).

It is well-known that ceria can affect (i) the thermal and structural stability of the catalyst carriers [32], (ii) the dispersion of supported metals [33], (iii) the facile oxidation and reduction of noble metals [34], (iv) oxygen storage and release characteristics of the composites [35] and (v) the decrease of carbonaceous formation on the catalyst surfaces [36]. The high oxygen storage/release capacity (OSC) is a result of high reducibility of Ce^{4+}, which is a consequence of high mobility of O^{2-} ions inside the ceria lattice [37]. Their use in the domain of catalysis is on the basis of superior chemical and physical stability, high oxygen mobility, and high oxygen vacancy concentrations, which are characteristics of fluorite-type oxides. The most important property of ceria is as an oxygen reservoir, which stores and releases oxygen via the redox shift between Ce^{3+} and Ce^{4+} under reducing and oxidizing conditions, respectively ($Ce^{3+} \leftrightarrow Ce^{4+}$) [38,39]. The possibility of cycling between reduced and oxidized states permit the reversible addition and removal of O_2 from the CeO_2. Ceria forms part of TWC formulations because it acts as an oxygen buffer by storing and releasing oxygen under controlled conditions. The Ce^{4+}/Ce^{3+} redox couples present in ceria containing catalysts is known to be responsible for this intrinsic property. In general, the TWCs are required to possess high thermal stability and mechanical strength, as they are located close to the engine. The high activity of cerium oxide in the redox reaction is attributed to the cerium oxide reducibility and its high oxygen vacancies. The catalytic activity of the ceria is greatly dependent on three main factors: particle size, structure distortion and chemical non-stoichiometry,

generally speaking reducing the particle size to nanoscale will provide a large number of more reactive sides.

1.3 Nanomaterials

Nanostructured materials are materials with a microstructure the characteristic length scale of which is on the order of a few (typically 1-100) nanometers. The microstructure refers to the chemical composition, the arrangement of the atoms (the atomic structure), and the size of a solid in one, two, or three dimensions. Effects controlling the properties of nanostructured materials include size effects (where critical length scales of physical phenomena become comparable with the characteristic size of the building blocks of the microstructure), changes of the dimensionality of the system, changes of the atomic structure, and alloying of components (e.g., elements) that are not miscible in the solid and/or the molten state. Nanophase or nanocrystalline ceramics are considered as very promising materials, both as intermediate-stage products offering good formability prior to sintering treatments, and as final stage products with enhanced mechanical properties for applications at low and intermediate temperatures and for functional properties. Nanophased materials of all types of materials are being considered for advanced applications for 21st Century. The synthesis, characterization and processing of *nanostructured materials* are part of an emerging and rapidly growing field. Research and developement in this field emphasizes scientific discoveries in the generation of materials with controlled microstructural characteristics, research on their processing into bulk materials with engineered properties and technological functions, and introduction of new device concepts and manufacturing methods. Nanomaterials have a particular distribution of crystallites or domains (in the case of an amorphous material) at a nanometer scale in a peculiar fashion. A strong macroscopic interaction occurs between the basic units of crystallites or domains. It determines the modified physical and chemical properties of nanostrucured materials. As the properties of solids depend on size, atomic structure, and chemical composition, nanostrucured materials exhibit new properties due to the following effects.

1. **Size effect**: Size effects result if the characteristic size of the building blocks of the microstructure (e.g. the crystallite size) is reduced to the point where critical length scales of physical phenomena (e.g. the mean free paths of electron or phonons, a

coherency length, a screening length, etc.) become comparable with the characteristic size of the building blocks of the microstructure.

2. **Change of the dimensionality of the system**: It occurs if a nanostrucured material consists of thin needle-shaped or flat two dimensional crystallites. Only two or one dimensional of the building blocks becomes comparable with the length scale of a physical phenomenon.
3. **Change of the atomic structure:** Changes in the atomic structure result if a high density of incoherent interfaces or other lattice defects such as dislocations, vacancies, etc., are incorporated.
4. **Alloying of components:** Large surface energy in small particles facilitates alloying or mixing even in immiscible solids.
5. **Temperature effects**: Elevated temperatures seem to affect the microstructure of nanostrucured materials by one or both of the following two types of processes.
6. **Grain growth**: Grain growth in nanostrucured materials is primarily driven by the excess energy stored in the grain or inter phase boundaries. Grain growth studies have been carried out by for various nanostrucured materials using TEM, DSC, X-ray diffraction and Raman spectroscopy. Several approaches for preventing grain growth have been proposed. Slow down the grain growth kinetics by reducing the driving force (the grain boundary free energy) or the grain boundary mobility.
7. **Temperature-induced variations of the atomic structure**: Materials with nanometer–sized microstructures may be classified according to their free energy into equilibrium nanostrucured materials and nanostrucured materials far away from thermodynamic equilibrium, which will be called "non-equilibrium NSMS". Properties altered by grain size include lowered thermal conductivity, increased hardness, and even low temperature ductility in some ceramics.

Nanocrystalline materials are characterized by their small crystallite size in the range of 2-20 nm, which are separated by their high angle grain or interface boundaries and, consequently, by their large volume fraction of disordered region of grain boundaries. The fraction of the surface atoms (φ) is a strong function of size and

morphology of the particle. Siegel performed a systematic analysis of φ as a function of average particle diameter <D> with different thickness for grain boundary. According to the special surface and σ the surface energy density, the surface atoms in an isolated particle of size of a nanometer scale in general assume

1. A lower atomic density,
2. A lower coordination number,
3. A lower symmetry, and
4. An enhanced interatomic distance

than those for the core atoms.

1.4 Drawbacks of Pure CeO_2 as a Catalyst

The major drawback of an oxygen storage system based on pure CeO_2 is related to its thermal resistance, low-temperature activity, and textural stability, which are not high enough to meet the requirements of high-temperature applications. So its use is highly discouraged as pure ceria is poorly thermostable [40,42]. The catalytic efficiency of ceria may be reduced at elevated temperatures because of sintering and loss of surface area. Sintering also causes a loss of oxygen storage capacity (OSC). The loss in surface area is usually related to changes in the pore structure and to crystallite growth. It is therefore essential to improve its textural stability. Therefore, much effort has been directed recently to find catalyst formulations that can enhance the thermal (textural) stability of CeO_2 without diminishing its special features, such as its unique redox properties and its high oxygen mobility. The preparation of ceria-containing materials with sufficiently high specific surface area is still not a well-known technology. Therefore, attempts to amplify the desired properties of ceria have been made although its electrical properties can be adjusted by doping with heterovalent cations; in the domain of catalysis, the formulations where ceria is spread over a thermally stable, high-surface area support or thoroughly mixed with other oxides have been synthesized and investigated. Ceria stabilized on alumina or silica has been found to be an efficient catalyst, especially for environmental applications such as combustion or removal of pollutants from auto-exhaust streams. For this reasons a strong effort has been directed to

increase the overall efficiency of CeO_2 in various applications and recently a new generation of mixed oxides based on CeO_2 and ZrO_2 has been developed. For the same reasons, special attention has been focused recently on the preparation of ceria-zirconia's solid solutions. Despite the fact that ceria-based mixed oxide systems have been widely investigated, there is still big interest in adjusting their properties that are important for catalytic applications.

1.5 Stabilization of CeO_2 Using ZrO_2 as a Dopant

Relative to ceria alone, ceria–zirconia mixed oxides are known to bear a high thermal resistance and increased OSC. Incorporation of zirconium into ceria leads to structural modification of the cubic fluorite structure of ceria that result in the decrease of the cell volume and activation energy for oxide ion diffusion [42]. A strong effort has been directed to increase the overall efficiency of ceria in these applications and recently a new generation of mixed oxides based on ceria and zirconia has been developed. The approach we used for the preparation of mesoporous, high surface area ceria-zirconia exploits the interaction of the mixture of hydrous oxides with surfactants under basic conditions. The method derives from the observation that hydrous oxide can exchange from either cations or anions, depending on the pH of the medium. It has been recently reported that hydrous zirconium oxide effectively incorporates cationic surfactants at a pH well above its isoelectric point, allowing a partial degree of ordering to develop over time [43]. The isoelectric point of hydrous zirconium oxide in aqueous solution is close to that of cerium and slightly dependent on the environment. In accordance with these features the following equilibrium can be delineated for Ce, Zr and a mixture of the two.

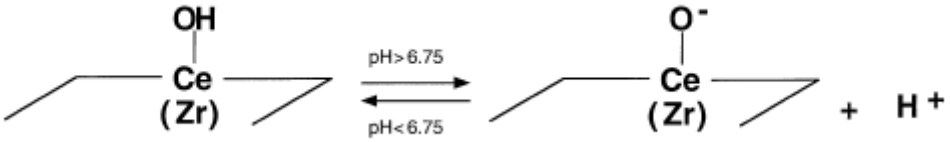

Conducting the precipitation of hydrous mixed oxide at a pH >8 in the presence of cationic surfactant should permit the cation exchange process between H^+ and the surfactant together with the formation of an inorganic/organic composite which upon

calcinations will originate a mesoporous mixed-oxide phase. The strong similarity of the isoelectric points of Zr and Ce would enable exchangeable sites to be equally distributed over the surface and the extent of substitution of the hydroxyl groups to be comparable. Their effectiveness derives from the improvement of several features with respect to catalysts based on pure ceria: ceria-zirconia shows enhanced redox and oxygen storage properties; improved thermal resistance; and better catalytic activity at lower temperatures. The preparation of compounds or solid solutions with many rare-earth elements and transition metals [42,44] has been attempted to overcome some of the previously mentioned disabilities of CeO_2. It easily forms solid solutions with other rare-earth elements and with elements belonging to the transition-metal series. Among rare-earth elements, CeO_2-Ln_2O_3 (Ln) La, Pr, Sm, Gd, and Tb) systems have been extensively investigated and their effects have been closely monitored. Regarding transition/non transition elements, CeO_2 easily forms solid solutions with ZrO_2, PbO_2, CuO, MnO_x, TiO_2, Al_2O_3, and SiO_2 and each has its own uniqueness.

Recent studies have suggested that formation of mixed oxides of ceria with cations such as Zr^{4+}, Al^{3+}, and La^{3+} enhances the catalytic, textural, redox, and oxygen storage properties of ceria and the so-formed mixed oxides also exhibit good thermal stability. Silica is a well-known support, which exhibits good chemical resistance, thermal stability, and high specific surface area. However, investigations on ceria-silica combination oxides are scarce in the literature. The redox and catalytic properties of CeO_2 are profoundly enhanced when used in combination with other transition metal or rare earth oxides. Among various elements, the introduction of zirconium into the ceria lattice has been particularly effective in the enhancement of the overall performance of CeO_2. In fact, ceria-zirconia mixed oxides have been regarded as potential substitutes for ceria in the formulation of new generation three-way catalysts (TWC) on the basis of their superior catalytic properties resulting from the combination of oxygen storage characteristics of ceria and superior refractory properties of zirconia. The ceria-zirconia mixed oxides exhibit several advantages [45] over pure ceria, which include high thermal resistance, improved reduction efficiency of the Ce^{4+}/Ce^{3+} redox couple, excellent oxygen storage/release capacity (OSC) and better catalytic activity at lower temperature. This was found to be due to the partial substitution of Ce^{4+} with Zr^{4+} in the lattice of

ceria, which results in a solid solution formation [46]. It was suggested that the role of zirconia is to control the structure or the sites of ceria crystallite. Many preparation methods have been applied for the preparation of CeO_2–ZrO_2 solid solution for catalytic applications. These include the high-temperature firing or high-energy milling of a mixture of the oxides conventional precipitation, and sol–gel techniques. Among these methods, sol–gel was found to be very beneficial since it yields products with high purity, homogeneity, well-controlled properties, and low temperature processing. The properties of the final products were found to be dependent on the temperature and the hydrolysis catalysts. One of the keys to this success is the selection of appropriate preparation methods and composition (i.e. Ce/Zr ratio), which in turn determine homogeneity at a molecular level and textural/morphological properties. Materials across almost the entire composition range with varying degrees of homogeneity and textural properties have been prepared. Generally, Ce-rich compositions are preferred for the purposes of catalysis and the best results are obtained using $Ce_xZr_{1-x}O_2$ with x ranging from 0.6 to 0.8. of course, textural properties also play an important role in the development of these materials, especially when they are used for the deposition of noble metals.

1.6 Phases of $Ce_{(1-x)}Zr_xO_2$

Depending on Ce/Zr atomic ratio and calcinations temperature, three different phases (cubic, monoclinic, or tetragonal) are frequently reported for $Ce_{(1-x)}Zr_xO_2$ solid solutions. Cubic phase normally dominates in the ceria rich compositions, whereas monoclinic is predominant in the zirconia-rich combinations. The metastable tetragonal phase also exists in a wide composition range (5-80 mol % Ce) when appropriate synthesis conditions are employed. Interestingly, the phase composition strongly influences the redox behavior of cerium oxide. Ceria belongs to the fluorite structure, and each O^{2-} anion is surrounded by a tetrahedron of Ce^{4+} cations located at the center of a cubic arrangement of equivalent O^{2-} ion. Insertion of smaller zirconium cations into ceria lattice leads to structural modification of the fluorite lattice. The resulting structural distortions facilitate high oxygen storage capacity (OSC), excellent thermal stability, and resistance to sintering.

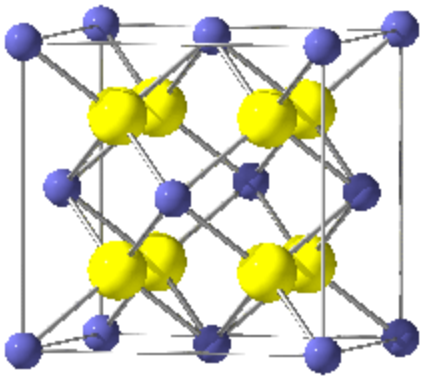

Fig. 1.1. *Cubic fluorite structure of CeO_2-ZrO_2 powders. The small circles are the cations and the big circles are anions.*

1.7 Porous materials

Porous materials are defined as solid containing pores. Generally speaking, porous materials have a porosity of 0.2-0.95. the porosity means the fraction of pore volume to the total volume. Pores are classified into two types open pores which connect to the outside of the material and closed pores which are isolated from outside and may contain a fluid. Introducing open pores in materials (producing open porous materials) changes material properties. Two essential changes are the decreased density and the increased specific surface area. Porous materials have pores (cavities, channels, interstices) which are deeper than they are wide. They are very important because of the ability of the pore wall to interact with atoms, ions or molecules. They can be used as substrates to support catalysts and can act as highly selective sieves that allow only certain molecules up to a particular size.

Porous materials are of scientific and technological importance because of the ability of the pore wall to interact with atoms, ions or molecules. These materials occur widely and have many important applications. They can be used as substrates to support catalysts and can act as highly selective sieves that allow only certain molecules up to a particular size. According to IUPAC convention, depending upon the pore size they can be classified into three classes as Microporous having pore size less than 2nm, mesoporous having pore size within 2nm to 50nm and Macroporous having pore size greater than 50nm.

1.7.1 Microporous materials

Microporous materials have pore diameters of less than 2 nm. They have narrow pore size distribution, this makes them to selectively allow some molecules to enter into pores and reject some other molecules that are either too large or have a shape that does not match with the pore size. A number of applications involving microporous materials utilize such size and shape selectivity. Micropore structure is closely connected to Type-1 BET isotherm. They have high specific strength and low thermal conductivity.

1.7.2 Mesoporous materials

According to IUPAC notation [47], microporous materials have pore diameters of less than 2 nm and macroporous materials have pore diameters of greater than 50 nm; the mesoporous category thus lies in the middle. Typical mesoporous materials include some kinds of silica and alumina that have similarly-sized fine mesopores. Mesoporous oxides of niobium, tantalum, titanium, zirconium , cerium and tin have also been reported. According to the IUPAC notation, a mesoporous material can be disordered or ordered in a mesostructure. The first mesoporous material, with a long range order, was synthesized in the late 80s/ early 90s, by a research group of the former Mobil Oil Company [1]. Since then, research in this field has steadily grown. Since 2007, a new type of porous particle was invented by Nandiyanto et al. in Hiroshima University. With his experience in preparing mesoporous particle with pore size of 30 nm, the particle with controllable pore size from 3 to 15 nm and outer diameter from 20 nm to 100 nm could be prepared by simple sol-gel preparation method. The assistance of surfactant/dual-polymerization was performed to obtain such kind porous particle. This material was named Hiroshima Mesoporous Material, or in abbreviation of HMM. Excellent properties were also demonstrated in a great adsorption of large molecule. Mesoporous materials are those with pores in the range 2-50 nm. Due to these small pore sizes mesoporous materials usually have very high surface area and other desirable properties like shape selectivity. They are used in catalysis, sorption, separation and microelectronics. They have amorphous structure rather than a crystalline structure. They show Type-IV BET isotherm. Mesoporous materials have got important optical applications. The high surface area creates the potential to dope materials at high concentrations. The mesosize range is attractive for producing size-confined structure. These materials are used for luminescent

sensors due to their high porous structure, low absorption and emission in the visible range.

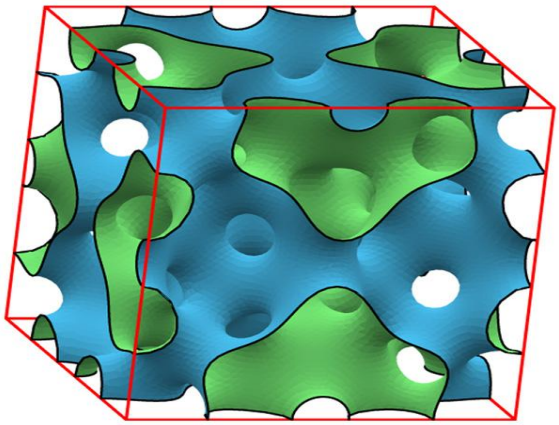

Fig. 1.2. *Mesoporous materials.*

1.7.3 Macroporous materials

These are materials containing pores with diameters greater than 50 nm. Macroporous materials have importance from the fields of adsorption-separation and heterogeneous catalysis because they have large internal surface area with the accessible diffusion pathways of macroporous network.

1.8 Role of surfactants

The incorporation of surfactant reduces tension of water even in the absence of a partial degree of ordering. As a matter of fact, surfactant can be added to the pore liquid to reduce the interfacial energy and thereby decreases the surface tension of water contained in the pores. This will reduce the shrinkage and collapse of the network during drying and calcinations, which could help to maintain high surface area. Surfactants are surface-active agents; they cover the surfaces of the small particles in colloidal suspensions and thus stabilize them. Various type of surfactants with different properties, anionic, cationic, zwitter ionic etc. are used to introduce the mesopores. Cationic surfactants give good stability over a range of pH levels. For controlling the pore size distribution sol-gel method is modified to a templated mechanism. Porous materials with uniform pore sizes were obtained by this method. Synthesis of pores up to 10 nm in diameter with surface areas up to 700 m^2/g can be achieved by using liquid crystal templating mechanism. The templating mechanism involves the dissolution of a surfactant

in the pre-hydrolysed inorganic precursor. The mechanism is influenced by the electrostatic and the steric interactions between the solvent molecules, the inorganic species and the self-assembled organic surfactants. The pore size can be controlled by the choice of surfactants. The lengthening of alkyl chain or addition of an auxiliary hydrocarbon results in an increase of pore diameter. Surfactants have unique ability to self organize at interfaces or in solution, modify interfacial properties and enhance the compatibility between materials of different characteristics.

The materials produced by templating mechanism have high surface area, high heat resistance and moisture resistance. So they are used in catalysis, sensors, adsorption, separation and electronic devices. Removal of surfactants can be done by calcination. The non-ionic templating approach allows the removal of surfactants by solvent extraction, as the hydrogen bonding involves is more easily broken. Other methods include plasma and super critical fluid extraction. Surfactant removal is also done by ozone. This involves highly exothermic process and cannot be controlled. The advantage of this method is that it forms large pores with a decreased size distribution and increased order.

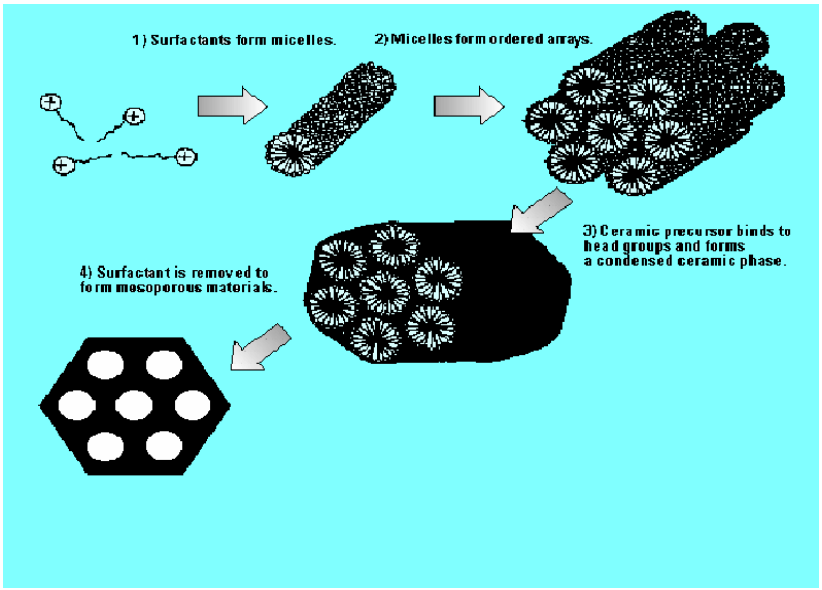

Fig. 1.3. *Schematic diagram showing the formation of mesoporous materials.*

1.9 Influence of p^H of the medium

Effective incorporation of the organic into the hydrous oxide is required for the surfactant to modify textural properties of the resulting oxide. Reaction conducted at a p^H of 8.5 for two days gives the highest surface area. At lower p^H values, the degree of incorporation of the surfactant is lower, owing to the presence of fewer surface OH groups, available for exchange. This will result in a less developed pore structure with a drop in surface area.

1.10 Influence of reaction time

The degree of incorporation of the surfactant and the homogeneity of solid solutions are also dependent on reaction times. Lower rection time will result in incomplete exchange reaction between the hydroxyl groups of the hydrous oxide and the surfactant.

CHAPTER-II
EXPERIMENTAL PROCEDURES & MEASUREMENTS

2.1 Objective of Present Work

- Synthesis of nanocrystalline porous CeO_2-ZrO_2 in powder forms using inorganic salts and dodecylamine (DDA) and sodium dodecyl sulfate **(*SDS*)** as surfactant.
- Study the effect of ZrO_2 addition on crystallite size of CeO_2-ZrO_2, and
- Structural characterization using X-Ray diffraction. SEM,TG-DTA & FTIR studies.

2.2 Synthesis Procedures

This chapter deals with a brief discussion of synthesis procedures of porous CeO_2-ZrO_2 powder.

2.2.1 with DDA Surfactant

Here, the starting materials are ammonium ceric nitrate and zirconium oxychloride. Zirconium oxychloride is used as the source of zirconia and ammonium ceric nitrate as the

source of ceria. Separate solutions of both these compounds are prepared in water. These two solutions are mixed with stirring. DDA in isopropanol was added slowly with vigorous stirring. The obtained solution was stirred and NH_4OH solution was added drop wise to get the precipitate (till pH becomes 8.5). Then this solution was kept for 2 days at room temperature. Then the precipitate was washed with distilled water to make it chlorine free. It was then filtered and washed, dried at 50°C for 24 hours on the water bath and powdered. The powder was calcined at different temperatures.

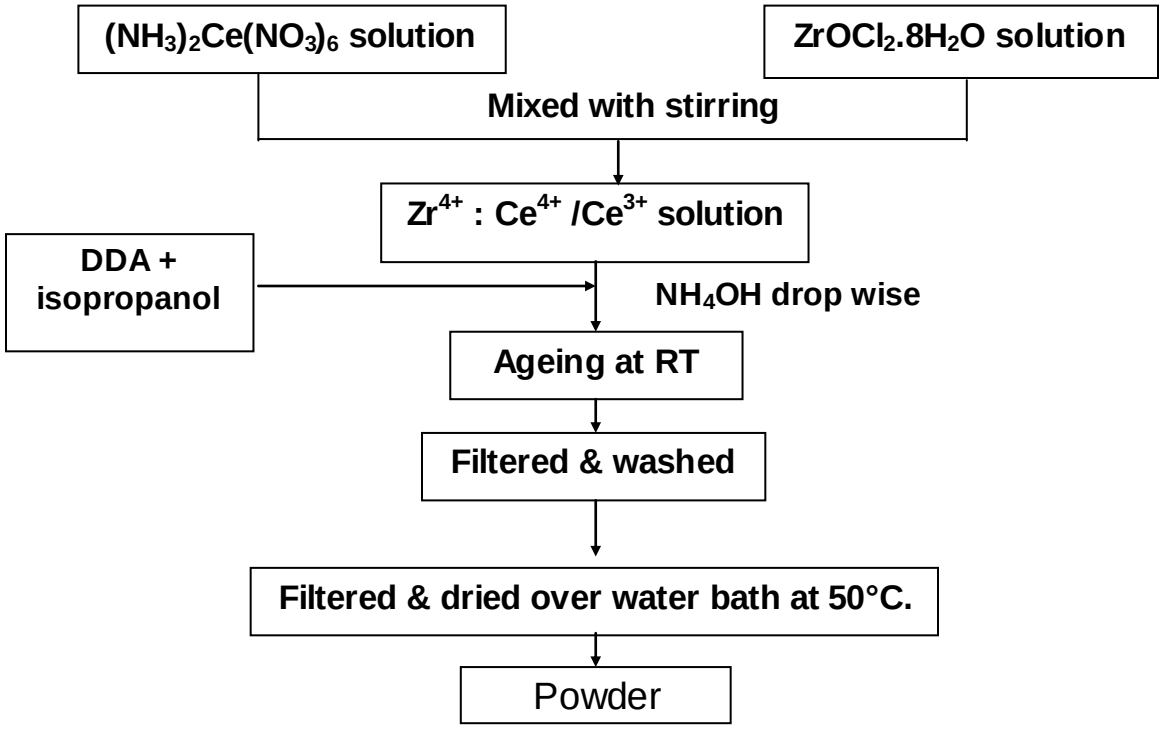

2.2.2 with SDS Surfactant

Similarly, porous CeO_2-ZrO_2 powders were prepared using aqueous solution of sodium dodecyl sulfate (SDS) instead of alcoholic solution of dodecylamine. All other procedures remain same.

2.2.3 without Surfactant

Similar process was followed to prepare sample without surfactant. But the adding of surfactant step was not done.

2.3 Characterization

The precursor and the porous powders were characterized by using X-Ray diffraction, FTIR and SEM and TG-DTA analysis. The CeO_2-ZrO_2 powders were prepared with DDA and SDS surfactant. The details of this method are discussed in the next pages.

2.3.1 X-Ray Diffraction

X-Ray Diffraction is used to perform phase analysis. The XRD analysis was performed by X-part APD, PW1830Gen, PW1050Gon and PW3710Con. The sample for this measurement was prepared by using a glass slide with a groove as the sample holder. The powder was placed in the groove and was compressed with the help of another glass slide. The excess powder was removed.

The sample at the flat surface at the slide was used to measure its characteristics X-ray diffraction pattern by using X-Ray diffractometer with the following set up,

Target - CuKα of wavelength λ= 0.1540 nm

Range of diffraction angle(2θ) - (20^0-80^0)

Scanning speed - 2^0/min

For a crystalline solid, the structure may be specific in terms of crystal unit cell and translations symmetry, the lattice leading to sharp Bragg peaks which are characteristic of the diffraction pattern of the crystalline solids. The structure of the amorphous solid, on the other hand, is characterized by a lack of symmetry, periodicity and long range order, resulting in a diffraction pattern. By using the XRD plot and Bragg's law the peaks were identified and subsequently phases were identified. Average crystallite size in the sample has been calculated from widths $\Delta 2\theta_{1/2}$ in characteristic diffraction peaks with the Debye –Schemer's formula, $D= 0.89\lambda/[(\Delta 2\theta_{1/2})\cos\theta_B]$, where $2\theta_B$ is the peak position in diffractogram.

2.3.2 Thermal and thermogravimetric analysis

Thermal decomposition/combustion of precursor mass into a dried CeO_2 - ZrO_2 ceramic powder is studied with thermogravimetry and differential thermal analysis (TG-DTA). The data are obtained by heating the sample at 20°C/min. The measurement is done by heating the specimen at a given heating rate in air atmosphere. The peak

positions in TG-DTA curve determine thermal decomposition and phase transformation or phase transition temperatures in precursor.

2.3.3 IR spectra

The IR spectrum was measured in the 400 to 4000 cm^{-1} region for sample dispersed in KBr pellets (in 10:90 ratio) with IR spectrophotometer. The reported values of frequencies are accurate to $\pm$ 2 cm^{-1} in the case of the sharp bands and $\pm$ 5 cm^{-1} or even larger in the case of the broad bands.

2.3.4 SEM

SEM measurements were carried out to investigate the detailed morphology, surface roughness and structure of the powders.

CHAPTER-III

RESULTS AND DISCUSSION

3.1 X-ray diffraction study

Figure 3.1 shows the X-ray diffractograms of pure CeO_2 prepared with and without surfactant and heated at 500°C. It shows single phase cubic fluorite structure. All the reflections of cerium (IV) oxide, which is corresponding to the cubic fluorite structure with space group *Fm*3*m* and lattice constant *a* = 5.4 Å, are observed. After applying the Scherrer formula to the (111) diffraction peak of cerium oxide, the crystallite size of cerium oxide nanoparticles are ~ 5 nm at 500°C. Sample with surfactant has broad peaks than that of without surfactant, as shown in Fig. 3.1b. This indicates that the sample with surfactant has smaller crystallite size than the samples prepared without surfactant.

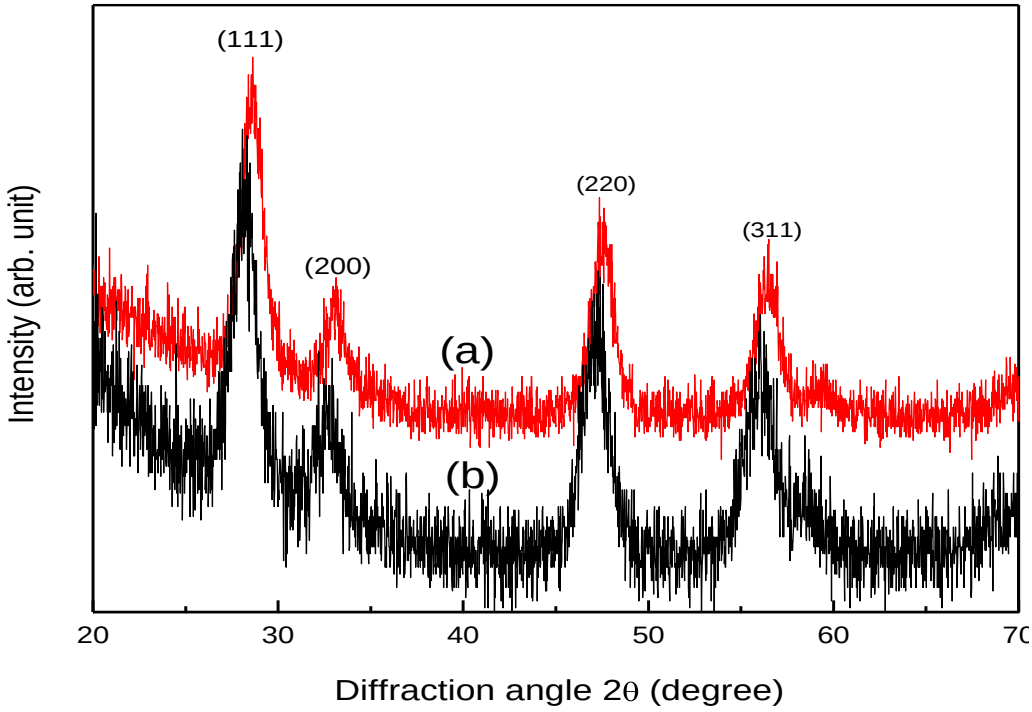

Fig. 3.1. X-ray diffractograms of pure CeO_2 nanopowders prepared (a) with and (b) without DDA, and heated at 500°C.

Figure 3.2 shows the X-ray diffractograms of 2 and 5 mol% ZrO_2 doped CeO_2 prepared with DDA surfactant and heated at 500°C. The peaks shows that it has single phase cubic fluorite structure. No peak coresponding to ZrO_2 arises up to as high content as 10 mol%. It has been observed that the peak broadening of (111) increases on increasing the ZrO_2 content in CeO_2. This is demostrated in Fig. 3.3. So, ZrO_2 plays important role in reducing

the crystallite size of CeO_2. The smallest particle size of 4 nm was observed in 10 mol% ZrO_2 doped in CeO_2.

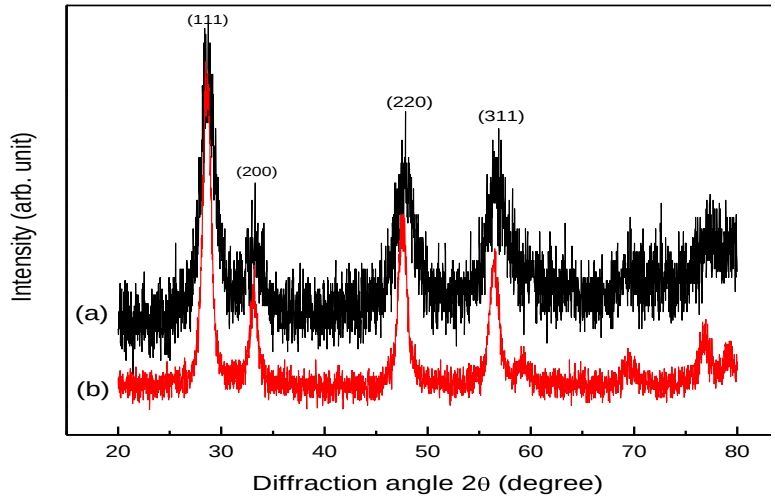

Fig. 3.2. X-ray diffractograms of (a) 2 and (b) 5 mol % ZrO_2 doped CeO_2 nanopowders prepared using DDA, and heated at 500°C.

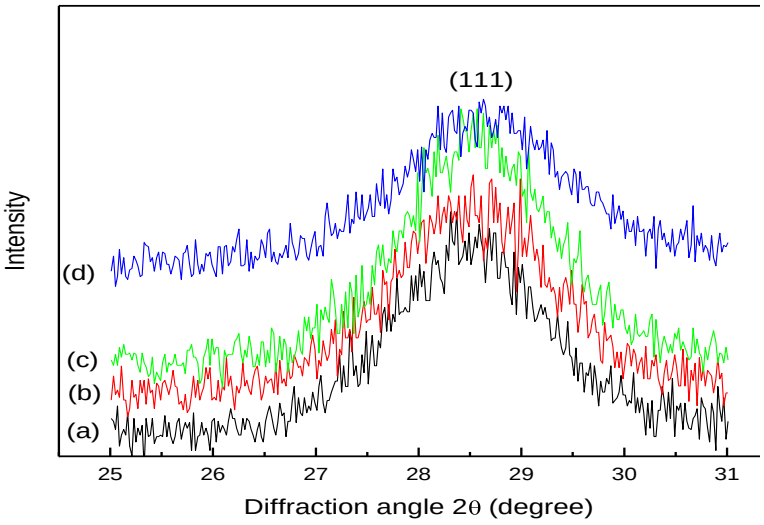

Fig. 3.3. X-ray diffractograms in (111) of (a) 0, (b) 2, (c) 5 and (d) 10 mol % ZrO_2 doped CeO_2 nanopowders prepared with SDS and heated at 500°C.

Figure 3.4 shows the X-ray diffractograms of 5 mol % ZrO_2 doped CeO_2 nanopowders prepared using SDS and heated at 500°C. It shows single phase cubic fluorite structure. It has been observed that the peak broadening of (111) increases on

addition of SDS instead of DDA, keeping the ZrO_2 content fixed at 5 mol%. This is demostrated in Fig. 3.5. So, ZrO_2 addition as well as the nature of surfactant used play important role in reducing the crystallite size of CeO_2.

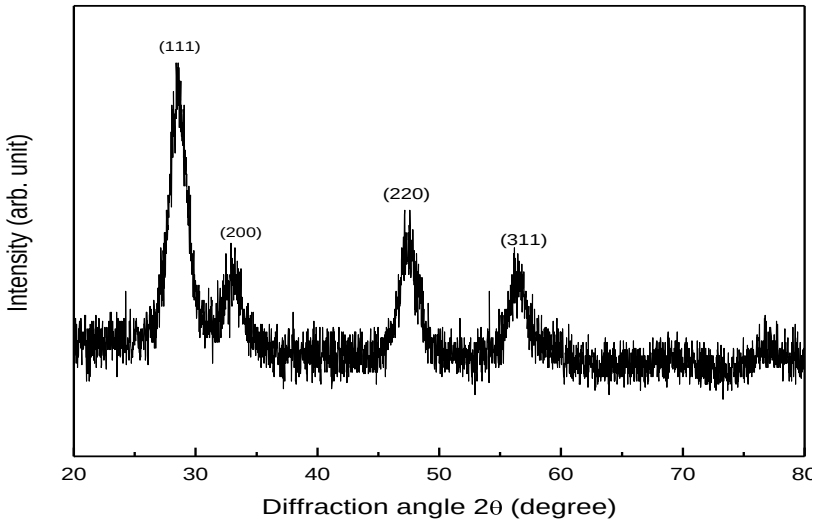

Fig. 3.4. X-Ray diffractograms of 5 mol % ZrO_2 doped CeO_2 nanopowders prepared using SDS and heated at 500°C.

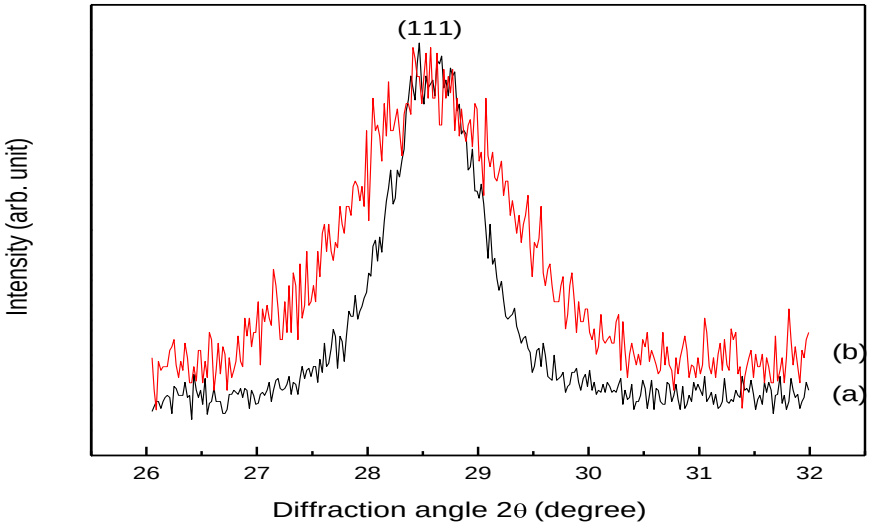

Fig. 3.5. X-Ray diffractograms of 5 mol % ZrO_2 doped CeO_2 nanopowders prepared using (a) DDA and (b) SDS and heated at 500°C.

3.2 IR Spectroscopic study

Figure 3.6 and 3.7 show IR spectra of as prepared sample synthesized using DDA and ZrO_2 doped CeO_2 nanopowders heated at 500°C. Peaks at 2959 and 2853 cm^{-1}

correspond to the C-H stretching of hydrocarbon bonds of DDA, which are very weak in as prepared sample. The peaks related to organic compounds are very weak in the CeO_2-ZrO_2 powders calcined at 500°C for 2 h. The results show that calcined samples are almost free from organic impurity. The broad band corresponding to –OH stretching recorded in the 3000 to 3500 cm^{-1} range. For as prepared sample, the peaks around 3370 cm^{-1} and 1621 cm^{-1} correspond to the O-H stretching and bending vibrations. For the calcined samples, the peak intensity is decreased compared to as prepared sample. The results demonstrate here that the calcined sample has adsorbed H_2O molecules on the surface of porous CeO_2-ZrO_2. The peak at 1520 cm^{-1} in as prepared sample is due to asymmetric stretching vibration of carbonyl group. The peak at 1335 cm^{-1} is due to the symmetric stretching of carbonyl group. The weak peak at 969 cm^{-1} is due to the presence of Ce-O-Zr bond. The peaks from 800 to 400 cm^{-1} are due to the presence of Ce-O bond.

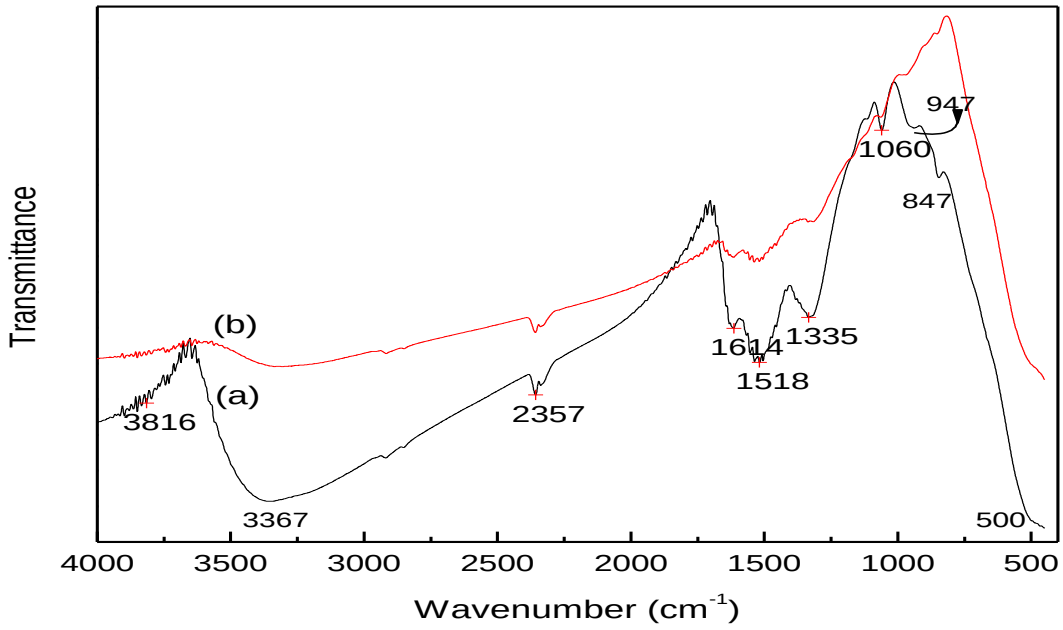

Fig. 3.6. IR spectra of (a) as prepared sample synthesized using DDA and (b) 2 mol% ZrO_2 doped CeO_2 nanopowder heated at 500°C.

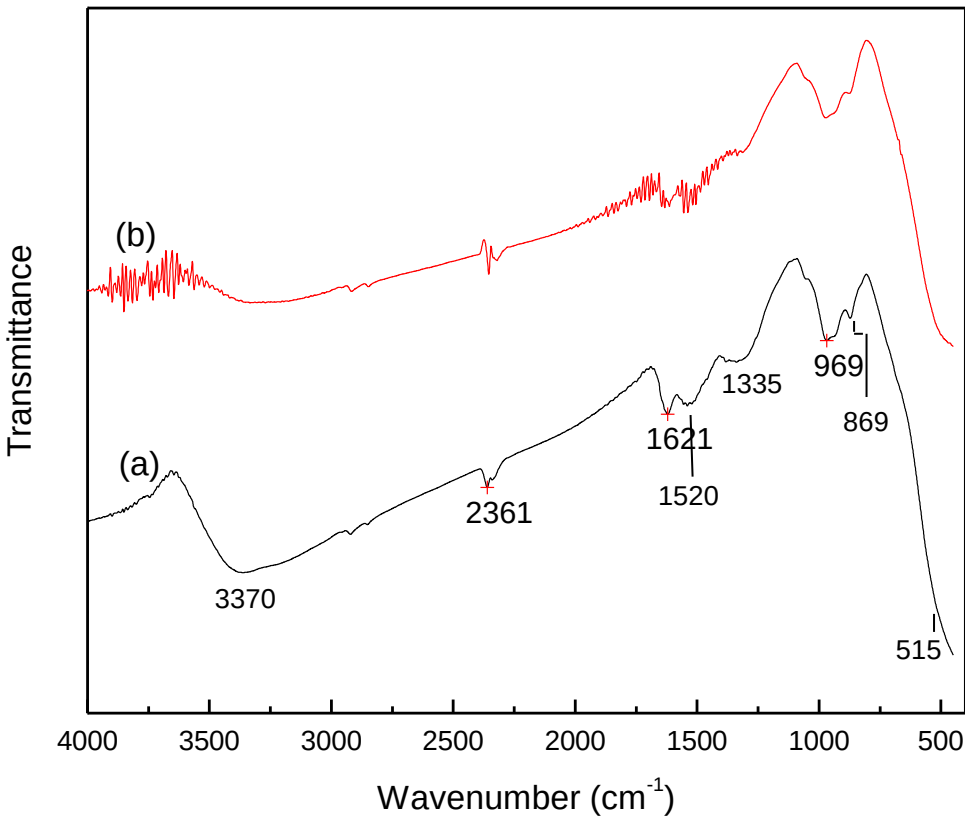

Fig. 3.7. IR spectra of (a) as prepared sample synthesized using DDA and (b) 10 mol% ZrO_2 doped CeO_2 nanopowder heated at 500°C.

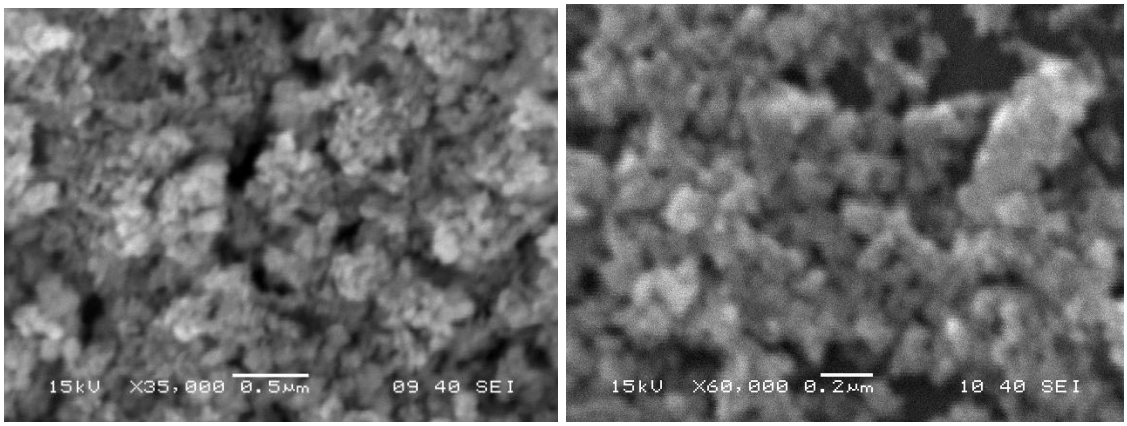

(a) (b)

Fig. 3.8. SEM images of (a)100CeO_2 and (b) 5 mol% ZrO_2 doped CeO_2 powder prepared using SDS and heated at 500°C.

3.3 SEM Analysis

From the SEM images in Fig. 3.8., it is clear that the prepared material is porous. The pores in black contrast are visible clearly. As the particle size/crystallite size is small, no much information is obtained from these image. It needs further characterization using TEM. The addition of surfactant induces the porous structure in CeO_2 doped ZrO_2 nanocrystals.

CHAPTER-IV

SUMMARY & CONCLUSION

- Mesoporous CeO_2-ZrO_2 nanopowders was synthesized in cubic fluorite structure which is stable up to as high as 500°C using inorganic salts of zirconium and cerium and cationic surfactants of DDA and SDS.
- Addition of ZrO_2 as well as the nature of surfactant used play important role in reducing the crystallite size of CeO_2.
- FTIR results show that mesoporous CeO_2-ZrO_2 nanopowders heated at 500°C is free from surfactant .
- SEM images shows that CeO_2-ZrO_2 nanopowders are porous in nature.

References:

1. C.T. Kresge, M.E. Leonowicz, W.J. Roth, J.C. Vartulli, J.S. Beck, Nature 359 (1992) 710–712.
2. M.E. Davis, Nature 364 (1993) 391–392.
3. J.Y. Ying, C.P. Mehnert, M.S. Wong, Angew. Chem. Int. Ed. Engl. 38 (1999) 56–77.
4. X. He, D.M. Antonelli, Angew. Chem. Int. Ed. Engl. 41 (2002) 214–229.
5. V.F. Stone, R.J. Davis, Chem. Mater.10 (1998) 1468–1474.
6. D.M. Antonelli, J.Y. Ying, Angew. Chem. Int. Ed. Engl. 34 (1995) 2014–2017.

7. M.P. Kapoor, Y. Ichihashi, K. Kuraoka, W.J. Shen, Y. Matsumura, Catal. Lett. 88 (2003) 83–87.
8. M. Vettraino, M.L. Trudeau, D.M. Antonelli, Adv. Mater. 12 (2000) 337–341.
9. M.S.Wong, E.S. Jeng, J.Y. Ying, Nano Lett. 1 (2001) 637–642.
10. R.K. Rana, L.Z. Zhang, J.C. Yu, Y. Mastai, A. Gedanken, Langmuir 19 (2003) 5904–5911.
11. Y. Zhou, D.M. Antonietti, J. Am. Chem. Soc. 125 (2003) 14960–14961.
12. A. Corma, P. Atienzar, H. Garcia, J.Y.C. Ching, Nat. Mater. 3 (2004) 394–397.
13. J.Y.C. Ching, F. Cobo, D. Aubert, H.G. Harvey, M. Airiau, A. Corma, Chem. Eur. J. 11 (2005) 979–987.
14. S. Deshpande, N. Pinna, B. Smarsly, M. Antonietti, M. Niederberger, Small 1 (2005) 313–316.
15. J.H. Ba, J. Polleux, M. Antonietti, M. Niederberger, Adv. Mater. 17 (2005) 2509–2512.
16. D.R. Rolison, Science 299 (2003) 1698–1701.
17. A. Trovarelli, Catal. Rev. Sci. Eng. 38 (1996) 439–520.
18. M. Flytzani-Stephanopoulos, MRS Bull. 26 (2001) 885–889.
19. A. Corma, J.M. Lo´pez-Nieto, in: K.A. Gschneider, Jr., L. Eyring (Eds.),Handbook on the Physics and Chemistry of Rare Earths, vol. 29, Elsevier,Amsterdam, 2000, p. 269 Chapter 185.
20. B.C.H. Steele, Solid State Ionics 129 (2000) 95–110.
21. E.P. Murray, T. Tsai, S.A. Barnett, Nature 400 (1999) 649–651.
22. A.J. Zarur, J.Y. Ying, Nature 403 (2000) 65–67.
23. J. Guzman, S. Carrettin, J.C. Fierro-Gonzalez, Y.L. Hao, B.C. Gates, A. Corma, Angew. Chem. Int. Ed. Engl. 44 (2005) 4778–4781.
24. D. Terribile, A. Trovarelli, J. Llorca, D. Leitenburg, G. Carla, Dolcetti, J. Catal. 178 (1998) 299–308.
25. D.M. Lyons, K.M. Ryan, M. Morris, J.Mater. Chem. 12 (2002) 1207–1212.
26. H.-W. Jen et al. / Catalysis Today 50 (1999) 309-328.
27. T. Ozaki, T. Masui, K. Machida, G. Adachi, T. Sakata, H. Mori, Chem. Mater. 12 (2000) 643.
28. M. Thammachart, V. Meeyoo, T. Risksomboon, S. Osuwan, Catal. Today 68 (2001) 53.
29. J. Huang et al. / Electrochemistry Communications 8 (2006) 785–789.

30. H. Takamura et al. / Solid State Ionics 179 (2008) 1354–1359.
31. Z.-Y. Yuan et al. / Catalysis Today 204 131 (2008) 203–210.
32. A. Piras et al. / Applied Catalysis B: Environmental 28 (2000) L77–L81.
33. M.C.J. Bradford, M. Albert Vannice / Catalysis Today 50 (1999) 87-96.
34. M.J. Tiernan, O.E. Finlayson / Applied Catalysis B: Environmental 19 (1998) 23-35.
35. A. Holmgren et al. / Applied Catalysis B: Environmental 22 (1999) 215–230.
36. S. Wang, G.Q. (Max) Lu / Applied Catalysis B: Environmental 19 (1998) 267-277.
37. B.M. Reddy et al. / Catalysis Today 110 141 (2009) 109–114.
38. J. Kaspar, P. Fornasiero / Journal of Solid State Chemistry 171 (2003) 19–20.
39. D. Terribile et al. / Catalysis Today 43 (1998) 79-88.
40. T.Yuzhakova,V. Ravic, C. Guimon, A. Auroux, Chem mater (2007), 19,2970-2981.
41. P. Fornasiero, G,Balducci, R. Di Monte, J. Kasper, V. Sergo, G. Gubitosa, A. Ferrero, M. Graziani, J. Catal. 164 (1996) 173.
42. B.M. Reddy, P. Bharali, P. Saikia, A. Khan, S. Loridant, M. Muhler, W. Gru¨ nert, J.Phys. Chem. C 111 (2007) 1878.
43. M.J. Hudson, J.A. Knowles, J. Mater. Chem. 6 (1996) 89.
44. B. K. Cho, J. Catal. 131(1991) 74.
45. C. E. Hori, H. Permana, K.Y.S. Ng, A. Brenner, K. More, K. M. Rahmoeller, D. N. Belton Appl. Catal. B 16 (1998) 105.
46. D. Terribile, A. Trovarelli, J. Liorca, C. de Leitenburg, G. Dolcetti, Catal. Today 43 (1998) 79.
47. J. Rouquerol et al., Pure & Appl. Chem, **66** (1994) 1739-1758.